Available online at www.worldscientificnews.com

World Scientific News

An International Scientific Journal

WSN 195 (2024) 210-220 EISSN 2392-2192

Performance Evaluation of Solubility Models for CO_2 Dissolved and Trapped during Sequestration

Bright Bariakpoa Kinate[1]*, Somiari Iyowuna Epelle[2]

[1]Department of Petroleum Engineering, Rivers State University, Nigeria
[2]Department of Petroleum and Gas Engineering, University of Port Harcourt, Nigeria
*Email address:baa2rex@yahoo.com

ABSTRACT

This work investigates the performance of two numerical solubility models for CO_2 dissolution and trapping. Two geological models were developed for Li-Nghiêm's and Harvey's solubility models. Visualization of the CO_2 plume's spatial distribution was conducted for 10-year injection period and plume migration monitored for 190 years under natural gradients. Both models successfully simulate the lateral migration of injected CO_2 during the injection phase, followed by upward migration due to its lower density relative to formation water. The onset of the solubility trapping mechanism results in a greater concentration of CO_2 at the bottom of the aquifer. There was structural trapping during the injection phase, followed by a slight increase and subsequent decline during the post-injection phase due to solubility trapping. Both models predict substantial CO_2 solubility in water during injection, but Li-Nghiêm's model have higher solubility than Harvey's model.CO2 solubility trapping mechanisms increased the concentration of CO_2 in the brine in the post-injection phase. it is evident that the choice of solubility model impact predictions of CO_2 solubility and migration and should be evaluated for any CO_2 storage Project. Hence, the selection should consider site-specific geological and fluid conditions.

Keywords: Li-Nghiem, Harvey, Solubility, Models, CO_2 Dissolved, CO_2 Trapped

(Received 26 June 2024; Accepted 15 July 2024; Date of Publication 29 July 2024)

1. INTRODUCTION

Carbon dioxide (CO_2) is the main greenhouse gas (GHG) which is the end product from the intake of fossil fuels which represent the primary energy source for industry and transport activities. Indisputably, the increase in CO_2 emission is related to sensible environmental issues such as the change in the climate and the increase of the global surface average temperature (Abas and Khan, 2014; Olajire, 2018; Venkatraman and Alsberg, 2017; Liu *et al.,* 2018; Singh, 2018). There has been a major area of interest within the ways to bring down the CO_2 level in the atmosphere, and one of these methods is to capture carbon and store it in the underground. This process is known as carbon capture and sequestration (CCS) (Soltanian *et al.,* 2016). CCS has been proven as the only way to decrease the CO_2 levels in the atmosphere. Technically, the carbon capture is made by means of cryogenic separation adsorption/absorption and membrane separation (Figueroa *et al.,* 2008), while one of the cutting-edge ways that getting much attention for the CO_2 sequestration is to inject it into deep saline aquifers (Gershenzon *et al.,* 2014; Gershenzon *et al.,* 2015).

To manage the sequestration of CO_2 in saline aquifers, it is required to have accurate representation of the brine and CO_2 related parameters (Dejam and Hassanzadeh, 2018; Bahadori *et al.,* 2009). CO_2 solubility in brine is considered the main parameter in the CO_2 sequestration in saline aquifers and its accurate prediction is necessary. Owing to the importance of CO_2 solubility in brine, numerous theoretical as well as experimental studies have been performed to deeply investigate a wide variety of related topics to this vital parameter.

The past few decades have seen rapid advances in developing correlations and thermodynamic paradigms to estimate properly the solubility of CO_2 in brine. The well-known thermodynamic models that were established over the past century are Li and Nghiem, (1986) and Zuo and Guo, (1991) models which are based on equations of state of Peng–Robinson and Patel–Teja, respectively. However, these models, and besides the limitation of their applicability domains, fail in providing accurate values of CO_2 solubility (Bahadori *et al.,* 2009). These lacks can be explained by the moderate varieties of data that were employed in the developments of these models. Recently, some other models have been introduced with the aim of predicting CO_2 solubility in brine, such as Sørensen *et al.,* (2002), Portier and Rochelle, (2005) and Duan *et al.,* (2006).

Cubic equations of state have been applied extensively to model the gas phase in phase equilibrium computations. However, for the aqueous phase, accurate prediction is difficult to achieve with an EOS. Henry's law is more appropriate to describe aqueous phase behavior for gas solubility in the aqueous phase. Furthermore, the Henry's law constant only depends on temperature and pressure, which makes computations more efficient. The two main models used to calculate the Henry's law constant were proposed by Harvey, (1996) and Li and Nghiem, (1986), respectively.

Sun, (2017) applied both of these models in his algorithm for gas solubility in water for EOR but did not consider the saline environment for the models. Therefore, this work seeks to evaluate CO_2 solubility in saline aquifer using both Harvey and Li and Nghiem models.

2. METHODOLOGY

2.1 Simulator and Data

Computer Modelling Group (CMG) and the following data ;Grid properties (Number of grid cells,Grid dimensions ,Permeability,Grid thickness,Depth to the top of reservoir, Rock physics functions(Relative permeability (saturations and phase relative permeabilities) ,Porosity,Rock compressibility,Fluid properties data,Compositional analysis of both the in-situ and injected fluid ,Brine properties),Well completion data(Well type,Trajectory and constraint, fluid and composition),Model initialization data(Reservoir temperature ,Reference pressure datum depth,Water gas contact) were used and presented in Table 1 to Table 6.

Table 1: Grid properties data

Properties	Value
Grid Top	1200m
Grid thickness	5m
Permeability (I, J and K)	100 millidarcies
Porosity	0.12
Rock compressibility	5.5e-7 per kPa
Reference pressure for rock compressibility	11800 kPa

Table 2: Data for GEM fluid model creation

Component	Mole fraction
CH4	0.999
CO2	0.001
Reservoir temperature for GEM fluid model	50°C

Table 3: Brine properties

Property	Value
Water density	1020kg/m^3
Water compressibility	4.35e-7 per psi
Reference pressure	11800kPa

Table 4: Water relative permeability data

Sw	Krw	Krow
0.2	0	1
0.2899	0.0022	0.6769
0.3778	0.018	0.4153
0.4667	0.0607	0.2178
0.5558	0.1438	0.0835
0.6444	0.2809	0.0123
0.7	0.4089	0
0.7333	0.4855	0
0.8222	0.7709	0
0.9111	0.95	0
1	0.9999	0

Table 5: Gas relative permeability data

Sg	Krg	Krog
0.0006	0	1
0.05	0	0.88
0.0889	0.001	0.7023
0.1778	0.01	0.4705
0.2667	0.03	0.2963
0.3556	0.05	0.1715
0.4444	0.1	0.0878
0.5333	0.2	0.037
0.6222	0.35	0.011
0.65	0.39	0
0.7111	0.56	0
0.8	0.9999	0

Table 6: Model initialization data

Properties	Value
Temperature	50°C
Reference pressure	11800 kPa
Datum depth	1200m
Water gas contact	1150m
CO2 fraction	0.001
CH4	0.999

2.2 Simulation Approach

GEM was used to set up an aquifer model and Builder was used for writing the dataset and validated with CMG-GEM. A two-dimensional (2D) homogeneous aquifer model of dimensions 100x1x20 (2000 grid blocks) and block width of 10ft both was developed. The model was populated with petrophysical, grid and rock properties using the data in Table 1. WINPROP, a CMG's compositional fluid modelling package was used to create a compositional fluid model required in the component section of CMG-GEM data file. The fluid model comprises of supercritical CO_2 and CH_4 in proportion of 0.001 and 0.999 (Table 2) with PR 1978 selected as the EoS for thermodynamic properties calculation. The CH_4 component was treated as the trace component.The Li-Nghiem's and Harvey's model were used for the calculation of Henry's constant for gas solubility in brine. The created fluid models were imported into the component section of GEM data file. Relative permeability data in Table 3 and 4 were used to define the relative permeability curves and the model was initialized using the data in Table 5. Water-Gas contact was set at 1150m above the reference depth which gave a model fully saturated with brine. Gas cap was initialized with supercritical CO_2 fraction of 0.001 and CH_4 fraction of 0.999 respectively. An injector well 'CO2_INJECTOR' was completed in three layers at the bottom of the model at 1298m, 1299m and 1300m. Pure supercritical CO_2 was injected at a maximum, constant surface gas rate of 10000m^3/day and maximum BHP of 44500kPa for 10years. The injector was shut-in after 10years of CO2 injection, with only natural gradient or density differences driving the flow for 190years. The simulation workflow is shown in Figure 1

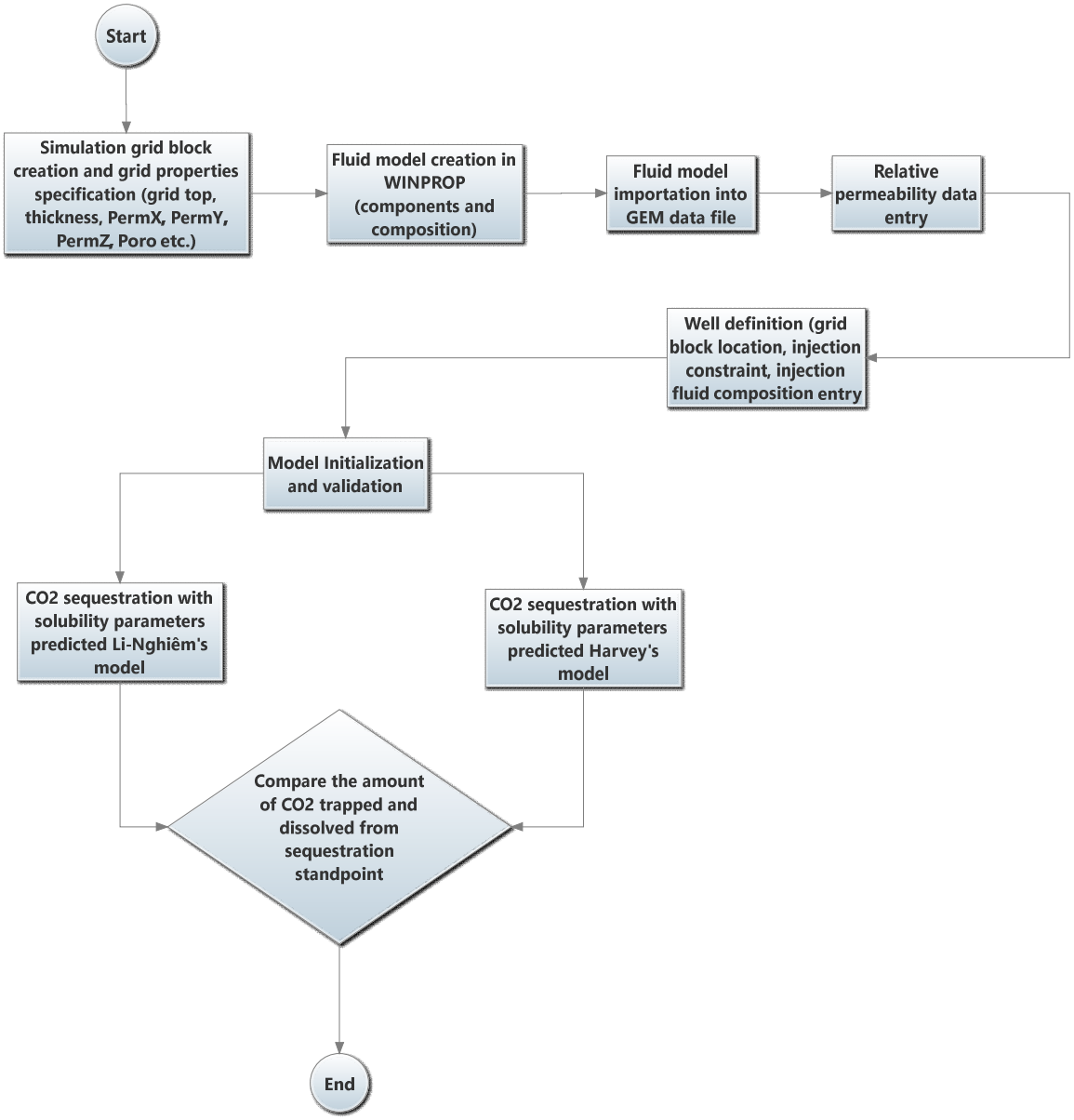

Figure 1: Simulation workflow

3. RESULTS

3.1 CO_2 solubility with Li-Nghiêms model

Figure 2 shows the spatial distribution of CO_2 plume with the Li-Nghiêm's method as the model for the calculation of Heny's constant for CO_2 solubility. Supercritical CO_2 was injected for 10years and the migration of the injected plume under the influence of natural gradients was monitored for 190 years.

The injected CO_2 migrated laterally during injection under the influence of pressure provided by the injection well. Post-injection, the lateral expansion of the plume ceased and CO_2 migrate upward due to its lighter density compare to formation water. There was a greater amount of CO_2 at the bottom of the aquifer as a result of the onset of solubility trapping mechanism. A gas cap of size 319.8672m was formed at the top of the structure with the Li-Nghiêm's model,.

Figure 2: 2D visualization CO_2 plume migration for Li-Nghiêm's model

The amount of CO_2 trapped structurally and dissolved in brine during the injection period and post-injection period with CO_2 solubility parameters calculated with the Li-Nghiêm's model is presented in figure 3.During the injection period, 11655107 moles of CO_2 were trapped structurally. Post-injection, the amount of CO_2 trapped structurally increases slightly before declined to a value 8578545 moles due to the onset of CO_2 solubility trapping mechanism. During the injection period, 12789660 moles of CO_2 was solubilized in water while during the post-injection period, CO_2 solubility trapping mechanism gave 26819612 moles of CO_2 in water.

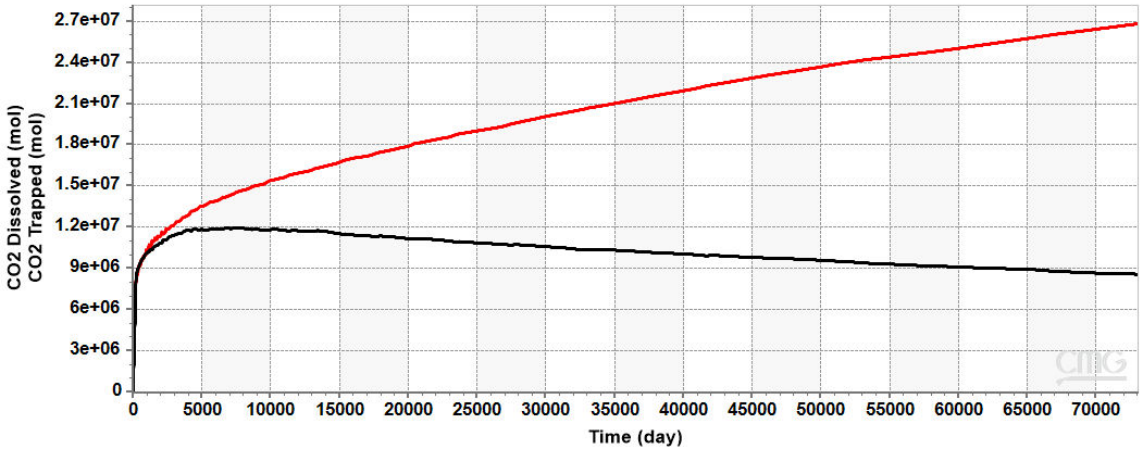

Figure 3: CO_2 structurally trapped and dissolved in brine for Li-Nghiêm's model

3.2 CO_2 solubility with Harvey's model

The spatial distribution of CO_2 plume with the Harvey's model for the calculation of CO_2 solubility parameters is shown in figure 4. CO_2 was injected for 10years and the migration of the injected plume under the influence of natural gradients was monitored for 190 years. The injected plume also migrated laterally during injection under the influence of pressure provided by the injection well. Post-injection, the lateral expansion of the plume cease and CO_2 migrate upward due to its lighter density. Result shows a greater amount of CO_2 at the bottom of the aquifer as a result of the onset of solubility trapping mechanism. For CO_2 solubility parameters calculated with the Harvey's model, a gas cap of size 320.2356m was formed at the top of the structure.

Figure 4: 2D visualization CO_2 plume migration for Harvey's model

The amount of CO_2 trapped structurally and dissolved in brine during the injection and post-injection periods with CO2 solubility parameters calculated with the Harvey's model is presented in figure 5. During the injection period, 11632032 moles of CO_2were trapped structurally.For Post-injection, the amount of CO_2 trapped structurally increases before declining to 8825584 moles due to the onset of CO_2 solubility trapping mechanism. During the injection period, 12517792 moles of CO_2 was solubilized in water while during the post-injection period, CO_2 solubility trapping mechanism gave 26449012 moles of CO_2 in water.

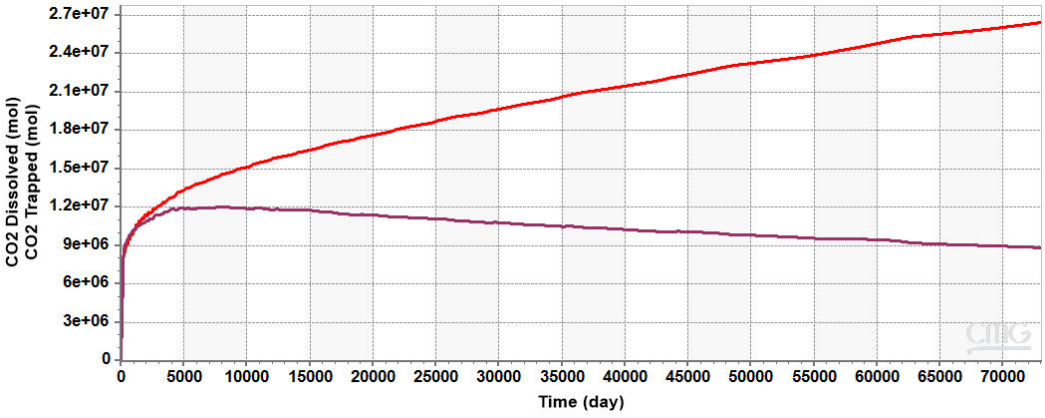

Figure 5: CO_2 structurally trapped and dissolved in brine for Harvey's model

3.3 Comparison of CO_2 structurally trapped and dissolved with both models

Figure 6 shows the amount of CO_2 solubilized in water with solubility parameters calculated with Li-Nghiêm's and Harvey's models. The Li-Nghiêm's model predicted a higher amount of CO_2 solubilized in water than Harvey's model. CO_2 solubility parameters calculated with Li-Nghiêm's model gave 26819612moles of CO_2 dissolved in brine while 26449012 moles of CO_2 was solubilized in brine with Harvey's models.

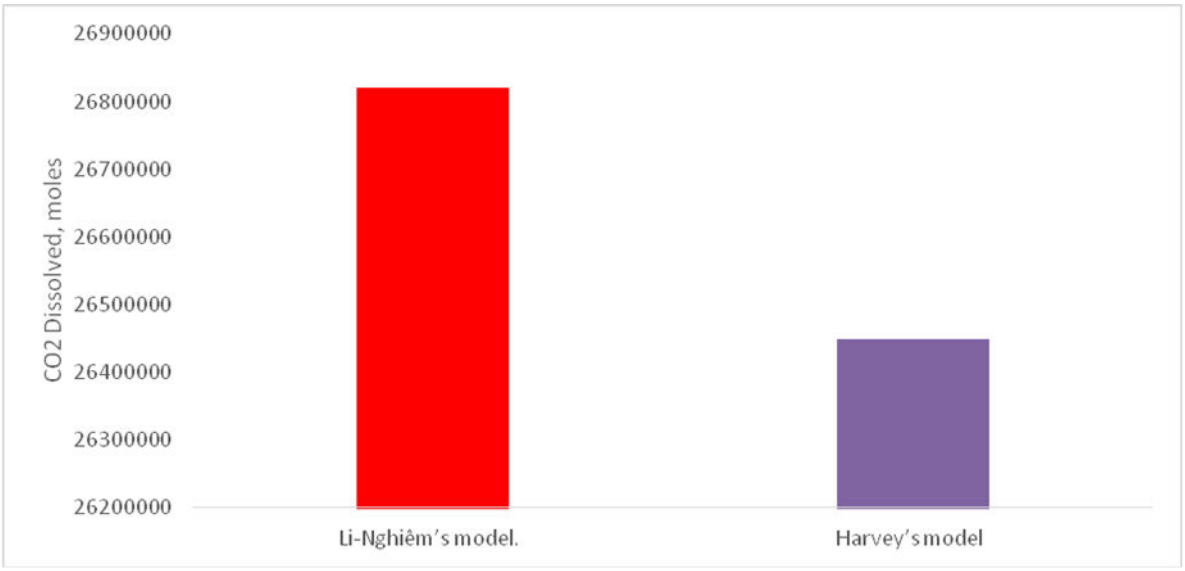

Figure 6: CO_2 solubility with Li-Nghiêm's and Harvey's models.

4. CONCLUSIONS

This work investigates the CO2 dissolved and trapped with two models by numerical simulation. Two models were developed for each method and solubility trapping mechanism of CO_2 in a geological storage simulated. Li-Nghiêm's model predicts a higher amount of CO_2 dissolved in brine than the Harvey's model. Both models resulted in the formation of a gas cap at the top of the geological structure. During the injection period, a substantial amount of CO_2 was structurally trapped in the geological formation. However, for post-injection, the amount of structurally trapped CO_2 declined in both scenarios due to the onset of the solubility trapping mechanism.

References

[1] Abas, N., and Khan, N. (2014). Carbon conundrum, climate change, CO2 capture and consumptions. *Journal of CO2 Utilization,* 8, 39–48.

[2] Bahadori, A., Vuthaluru, H. B., and Mokhatab, S. (2009). New correlations predict aqueous solubility and density of carbon dioxide, *International Journal of Greenhouse Gas Control,* 3, 474–480.

[3] Dejam, M., and Hassanzadeh, H. (2018). The role of natural fractures of finite double-porosity aquifers on diffusive leakage of brine during geological storage of CO2. *International Journal of Greenhouse Gas Control,* 78, 177–197.

[4] Duan, Z., Sun, R., Zhu, C., and Chou, I. M. (2006). An improved model for the calculation of CO2 solubility in aqueous solutions containing Na+, K+, Ca2+, Mg2+, Cl-, and SO42-. *Marine Chemistry,* 98, 131–139.

[5] Figueroa, J. D., Fout, T., Plasynski, S., McIlvried, H., and Srivastava, R. D. (2008). Advances in CO2 capture technology—the US department of energy's carbon sequestration program, *International Journal of Greenhouse Gas Control,* 2, 9–20.

[6] Gershenzon, N. I., Ritzi, R. W., Dominic, D. F., Soltanian, M., Mehnert, E., Okwen, R. T. (2015). Influence of small-scale fluvial architecture on CO2 trapping processes in deep brine reservoirs. *Water Resources Research*, 51, 8240–8256.

[7] Gershenzon, N. I., Soltanian, M., Ritzi Jr, R. W., and Dominic, D. F. (2014). Influence of small-scale heterogeneity on CO2 trapping processes in deep saline aquifers. *Energy Procedia,* 59 166–173.

[8] Harvey, A. H. (1985). The prediction of the solubility of gases in water and in aqueous-electrolyte solutions. Journal of the Chemical Society, Faraday Transactions 1, 81(4), 717-734.

[9] Harvey, A. H. (1996). Semiempirical correlation for henry's constants over large temperature ranges. *AIChE Journal,* 42(5), 1491–1494.

[10] Harvey, A. H., and Prausnitz, J. M. (1989). Carbon dioxide solubility in aqueous alkanolamine solutions. *Industrial & Engineering Chemistry Research*, 28(11), 1703-1710.

[11] Li, Z., & Nghiem, L. D. (2010). Modeling of CO2 solubility in saline water. Energy Procedia, 4, 5871-5878.

[12] Liu, B., Fu, X., and Li, Z. (2018). Impacts of CO2-brine-rock interaction on sealing efficiency of sand caprock: a case study of Shihezi formation in Ordos basin. *Advances in Geo-Energy Research,* 2, 380–392.

[13] Olajire, A. A. (2018). Recent progress on the nanoparticles-assisted greenhouse carbon dioxide conversion processes. *Journal of CO2 Utilization,* 24, 522–547.

[14] Portier, S., and Rochelle, C. (2005). Modelling CO2 solubility in pure water and NaCl-type waters from 0 to 300 C and from 1 to 300 bar: application to the Utsira Formation at Sleipner. *Chemical Geology,* 217, 187–199.

[15] Singh, H. (2018). Impact of four different CO2 injection schemes on extent of reservoir pressure and saturation. *Advances in Geo-Energy Research,* 2, 305–318.

[16] Soltanian, M. R., Amooie, M. A., Cole, D. R., Graham, D. E., Hosseini, S. A., Hovorka, S., Pfiffner, S. M., Phelps, T. J., and Moortgat, J. (2016). Simulating the Cranfield geological carbon sequestration project with high-resolution static models and an accurate equation of state, *International Journal of Greenhouse Gas Control,* 54, 282–296.

[17] Sørensen, H., Pedersen, K. S., and Christensen, P. L. (2002). Modeling of gas solubility in brine. *Organic Geochemistry,* 33, 635–642.

[18] Sun, R. (2017). Multiphase Equilibrium Calculations with Gas Solubility in Water for Enhanced Oil Recovery. Master degree thesis, University of Stanford.

[19] Venkatraman, V., and Alsberg, B. K. (2017). Predicting CO2 capture of ionic liquids using machine learning. *Journal of CO2 Utilization,* 21, 162–168.

[20] Zuo, Y. X., and Guo, T. M. (1991). Extension of the Patel Teja equation of state to the prediction of the solubility of natural gas in formation water. *Chemical Engineering Science,* 46, 3251–3258.